BIOCHEMICAL PHARMACOLOGY 73 (2007) 954–963

available at www.sciencedirect.com

ScienceDirect

journal homepage: www.elsevier.com/locate/biochempharm

Biochemical and pharmacological characterization of P-site inhibitors on homodimeric guanylyl cyclase domain from natriuretic peptide receptor-A

Simon Joubert, Normand McNicoll, André De Léan *

Department of Pharmacology, Faculty of Medicine, Université de Montréal, Montréal, Québec, Canada H3T 1J4

ARTICLE INFO

Article history:
Received 7 September 2006
Accepted 7 December 2006

Keywords:
Guanylyl cyclase
Natriuretic peptide
P-site inhibitor
Nucleotide
Purine
Catalysis
Protein dimer

ABSTRACT

Guanylyl cyclases catalyze the formation of cGMP from GTP. This family of enzymes includes soluble (sGC) and particulate guanylyl cyclases (pGC). The sGC are heterodimers containing one active catalytic site and one inactive pseudo-site. They are activated by nitric oxide. The pGC are homodimers whose activity is notably regulated by peptide binding to the extracellular domain and by ATP binding to the intracellular kinase homology domain (KHD). The catalytic mechanism of the pGC is still not well understood. Homology modeling of the structure of the homodimeric guanylyl cyclase domain, based on the crystal structure of adenylyl cyclase, suggests the existence of two functional sites for the substrate GTP. We used a purified and fully active recombinant catalytic domain from mammalian pGC, to document its enzyme kinetics properties in the absence of the KHD. The enzyme presents positive cooperativity with the substrate Mg-GTP. However, a heterodimeric catalytic domain mutant (GC-HET) containing only one active catalytic site is non-cooperative and is more similar to sGC. Structure–activity studies of purine nucleoside analogs indicate that 2′d3′GMP is the most potent inhibitor of pGC tested. It displays mixed non-competitive inhibition properties that are potentiated by the second catalytic product inorganic pyrophosphate (PPi). It appears to be equivalent to purinergic site (P-site) inhibitors characterized on particulate adenylyl cyclase. Inhibition of pGC by 2′d3′GMP in the presence of PPi is accompanied by a loss of cooperative enzyme kinetics. These results are best explained by an allosteric dimer model with positive cooperativity for both the substrate and inhibitors.
© 2006 Elsevier Inc. All rights reserved.

1. Introduction

Guanylyl cyclases are a family of enzymes that catalyze the formation of 3′,5′-cyclic GMP from GTP. In mammalian systems, two general topological variants of the enzyme are found. Soluble guanylyl cyclases (sGCs) are heterodimers composed of α and β subunits. Each subunit contains an N-terminal regulatory heme binding domain, a dimerization

* *Corresponding author*. Tel.: +1 514 343 6931; fax: +1 514 343 2291.
E-mail address: delean@pharmco.umontreal.ca (A. De Léan).

Abbreviations: sGC, soluble guanylyl cyclase; pGC, particulate guanylyl cyclase; PPi, inorganic pyrophosphate; 2′d3′GMP, 2′-deoxy-3′-guanosine monophosphate; 2′d5′AMP, 2′-deoxy-5′-adenosine monophosphate; 2′d5′GMP, 2′-deoxy-5′-guanosine monophosphate; 2′5′dd3′AMP, 2′5′-dideoxyadenosine-3′-monophosphate; GC-A, guanylyl cyclase A; NPR-A, natriuretic peptide receptor-A; GC-C, guanylyl cyclase C or guanylin/enterotoxin receptor; ANP, atrial natriuretic peptide; GC-E, guanylyl cyclase E; retGC-1, retinal guanylyl cyclase; KHD, kinase homology domain; k_{cat}, catalytic constant; $S_{0.5}$, Michaelis–Menten constant; K_i, inhibition or dissociation constant of inhibitor; V_{max}, maximal enzyme activity

0006-2952/$ – see front matter © 2006 Elsevier Inc. All rights reserved.
doi:10.1016/j.bcp.2006.12.008

domain and a C-terminal catalytic domain. Enzyme activity is greatly enhanced by binding of nitric oxide to the N-terminal regulatory domain [1]. The subunits are only partly homologous and they contain complementary mutations in key residues of their catalytic sites, such that only one site is active, while the other pseudo-site is inactive, but could bind purine nucleotides and other allosteric molecules [2–4].

In particulate guanylyl cyclases (pGCs), a single transmembrane domain divides the molecule into an extracellular ligand binding domain and an intracellular region containing a protein kinase homology domain (KHD), an amphipathic coiled-coil and a guanylyl cyclase catalytic domain, with a C-terminal extension for several specific isoforms. Seven genes for pGCs are found in mammals [5]. All mammalian pGCs are believed to function as homodimers or homo-oligomers [5]. Invertebrate guanylyl cyclases are numerous. They are involved in neuronal signalling and display atypical properties [6,7].

sGCs and pGCs both produce cGMP and have ~50% catalytic domain sequence identity [8]. But modeling and comparison of their catalytic domain structures suggests that, contrary to the sGCs which contain only one functional GTP binding site, pGCs would contain two potentially functional GTP binding sites [8]. In agreement with this concept, enzyme kinetics for pGC typically displays positively cooperative behaviour, especially in the presence of Mn^{2+}. However, in the case of both sGC and pGC, no crystallographic data has been reported yet and current models are solely derived by homology modeling with adenylyl cyclase structure.

Direct inhibition of adenylyl cyclase by purine nucleotides (P-site inhibitors) has been previously documented. Some purine nucleotides act as substrate analogs that mainly compete with the substrate at the catalytically active site in its free state. Other agents termed P-site inhibitors have been extensively studied [9–11]. These inhibitors are generally non-competitive or uncompetitive, suggesting that they might bind to the post-transition state of the enzyme. Their potency is typically increased in the presence of the second catalytic product inorganic pyrophosphate. Some of the most potent P-site inhibitors are 2′,5′-dideoxyadenosine-3′-mono- and 3′-polyphosphates [12]. Structural and functional studies have lead to an elegant model for their action. According to those studies, P-site inhibitors bind directly to the active catalytic site in replacement for the main product 3′,5′-cyclic-AMP and prior to the release of the other product inorganic pyrophosphate [13,14]. This would result in a product dead end inhibition mechanism, which could explain the mixed-competitive behaviour of these inhibitors. Initial results have documented that the heterodimeric sGC, which is more analogous to adenylyl cyclase than pGC, can also be inhibited by the corresponding agent 2′d3′GMP [15]. However, no structure–activity relationships or enzyme kinetics studies of P-site inhibitors for the homodimeric pGC have been reported. Since both sites for pGC are presumably functional and equivalent, this suggests that more complex inhibitory mechanisms involving site–site interactions might be involved for pGC.

In this report, we aimed to characterize the catalytic activity of the purified guanylyl cyclase homodimeric domain of pGC from the natriuretic peptide receptor-A (NPR-A or GC-A) in the absence of the KHD which also binds purine nucleotides, and to study the properties of P-site inhibitors and substrate analogs for this enzyme. The results indicate that positive cooperativity is observed with the natural substrate Mg-GTP. This cooperativity requires both catalytic sites to be functional. In addition, P-site inhibitors display mainly competitive inhibition, an effect that is potentiated by the second catalytic product pyrophosphate (PPi). Positive cooperativity is countered by the presence of P-site inhibitors and PPi. The results are consistent with a dimeric cooperative model for which the substrate and the inhibitor could bind to both catalytic sites of homodimeric pGC.

2. Materials and methods

2.1. Materials

2′d5′GMP, 2′d3′GMP, 2′d5′AMP, 2′AMP, 3′AMP, 2′5′dd3′AMP, 2′3′-dideoxyadenosine, 5′ATP, 5′AMP, 5′GMP, 5′GTP, PPi and guanosine 3′5′cGMP were from Sigma–Aldrich (Oakville, Ont., Canada). Guanosine and guanosine 2′,(3′)-monophosphate (a mixture of the 2′- and 3′-isomers of GMP) were from MP Biomedicals (Solon, OH, USA) and 2′,3′-dideoxyguanosine was from Axxora (San Diego, CA, USA).

2.2. Plasmid constructs and site-directed mutagenesis

Mammalian expression vector containing the rat NPR-A was the same as previously reported [16]. The guanylyl cyclase catalytic domain of NPR-A (GC-A) (amino acids Asn^{776} to Gly^{1029}) was amplified using the following strategy: PCR was done with two sense primers made of an excess (25 pmol) of 5′-AAAAGAATTCAACATGAACCATCACCATCACCATCACAAC-3′ and a limiting amount (250 fmol) of 5′-CCATCACCATCACCATCACAACAGCAGCAACATCCTGGACAAC-3′ and one antisense primer (5′-TTTTGGTACCTCAGCCTCGAGTGCTACATCC-3′) to introduce an *Eco*RI restriction site followed by six histidine residues at the N-terminal, and a *Kpn*I restriction site after the C-terminal stop codon. The *Eco*RI/*Kpn*I co-digested fragment was ligated into the pFastBac1 vector (Invitrogen) to obtain the GC-WT construct. The $D^{849}A$ mutated protein was obtained using the QuickChange method (Stratagene) with two mutant oligonucleotides (5′-GTTACCATCTACTTCAGTGCTATTGTGGGCTTTACAGCTC-3′ and 5′-GAGCTGTAAAGCCCACAATAGCACTGAAGTAGATGGTAAC-3′). The $N^{968}S$ mutation was obtained using the same method (5′-CTCTTTGGAGACACAGTCAGCACAGCTTCAAGAATGGAG-3′ and 5′-CTCCATTCTTGAAGCTGTGCTGACTGTGTCTCCAAAGAG-3′). The histidine-tag of the $N^{968}S$ mutated protein was then replaced by a Protein C epitope (EDQVDPRLIDGK) using the following strategy: PCR was done with two sense primers made of an excess (25 pmol) of 5′-AAAAGAATTCAACATGGAGGACCAGGTCGATCCGCGTCTGATTGATGG-3′ and a limiting amount (250 fmol) of 5′-CGATCCGCGTCTGATTGATGGCAAGAACAGCAGCAACATCCTGGACAACC-3′ and one antisense primer (5′-TTTTGGTACCTCAGCCTCGAGTGCTACATCC-3′). The *Eco*RI/*Kpn*I co-digested fragment was ligated into the pFastBac1 vector (Invitrogen) to obtain the GC-$N^{968}S$ construct. Sequences were confirmed using automated nucleic acid sequencing. Constructs with pFastBac1 were transformed in DH10Bac bacteria to obtain recombinant

bacmid DNA according to the Invitrogen. baculovirus expression system.

2.3. Transfection of Sf9 insect cells and titration of recombinant baculovirus by protein expression

Sf9 cells were grown in SF-900 II SFM medium (Gibco) containing penicillin and streptomycin on a rotating shaker at 28 °C. For each transfection, 9×10^5 cells were seeded in a six-well plate and allowed to attach for at least 1 h. Recombinant bacmid DNA was transfected into Sf9 insect cells using Cellfectin reagent as described for the pFastBac baculovirus expression system (Invitrogen). In order to maximize the expression levels of GC's in Sf9 cells, we tested the ratio of recombinant baculovirus over Sf9 cells by sequential dilution. Briefly, Sf9 cells (2×10^6) were plated in 35 mm petri dishes and increasing amounts of recombinant baculovirus were added. After 72 h, medium was removed and cells were washed once with PBS, resuspended in Laemmli sample buffer and submitted to electrophoresis as described below. After the Western blot (see below), bands corresponding to the protein of interest were evaluated by densitometry. The dilution corresponding to the maximum level of expression was used to scale up the production of GCs.

2.4. Expression of guanylyl cyclase in Sf9 cells

Sf9 cells (5×10^7) were incubated in 100 mL of SF-900 II SFM medium in a 250 mL Erlenmeyer flask on a rotating shaker for 48 h at 28 °C. Typically, 1 mL of recombinant baculovirus was added and the incubation was prolonged for another 72 h. Then, Sf9 cells (2×10^8) expressing GC-WT, GC-N^{968}S and the heterodimer GC-D^{849}A-N^{968}S were centrifuged at $500 \times g$ for 5 min and washed twice with PBS. Cells were homogenized using a polytron in 40 mL of 50 mM $NaPO_4$, pH 7.4, 300 mM NaCl, 0.1 mM EDTA, 1 μM aprotinin, 1 μM leupeptin, 1 μM pepstatin and 10 μM Pefabloc. After centrifugation at $40{,}000 \times g$ for 30 min, cytosolic fraction was passed through a 0.22 μm filter and kept at 4 °C until use. For Sf9 cells expressing GC-D^{849}A, homogenization was performed in 40 mL of 20 mM Tris–HCl, pH 7.5, 100 mM NaCl containing protease inhibitors and processed as described above.

2.5. Purification of guanylyl cyclase catalytic domain

GC-WT, GC-N^{968}S and the heterodimer GC-D^{849}A-N^{968}S, which all contain a histidine-tag, were purified on Ni-NTA agarose as follows: after addition of 15% glycerol and 20 mM imidazole, each cytosolic fraction was loaded on a 1 mL Ni-NTA column. The gel was washed with 10 mL of 50 mM $NaPO_4$, pH 7.4, 300 mM NaCl, 0.1 mM EDTA, 20 mM imidazole and the GC was eluted with 10 mL of 50 mM $NaPO_4$, pH 7.4, 300 mM NaCl, 0.1 mM EDTA, 200 mM imidazole and collected in fractions of 1 mL. Typically the guanylyl cyclase eluted from Ni-NTA column in fractions 2 and 3 as determined by immunoblot analysis.

GC-D^{849}A and the heterodimer GC-D^{849}A-N^{968}S (previously purified on Ni-NTA and dialyzed against 20 mM Tris–HCl, pH 7.5, 100 mM NaCl) both containing the Protein C epitope were purified on anti-Protein C agarose as follows: after addition of 10% glycerol and 1 mM $CaCl_2$, each preparation was loaded on a 1 mL anti-Protein C column. The gel was washed with 10 mL of 20 mM Tris–HCl, pH 7.5, 100 mM NaCl, 1 mM $CaCl_2$ and eluted at 22 °C with 6 mL of 20 mM Tris–HCl, pH 7.5, 100 mM NaCl and 10 mM EDTA and collected in fractions of 1 mL. In these conditions, guanylyl cyclase eluted from the anti-Protein C column in fraction 2.

2.6. Steric exclusion HPLC

GC-WT, GC-D^{849}A and GC-N^{968}S were further purified by steric exclusion chromatography on Superose-12, while the heterodimer GC-D^{849}A-N^{968}S (purified by the two sequential affinity chromatography steps) was tested for its purity and monitored for its exclusion volume on the same column. Chromatography on the Superose-12 was performed at 4 °C in 50 mM $NaPO_4$, pH 7.4, 300 mM NaCl and 0.1 mM EDTA with a flow rate of 0.5 mL/min. Optical densitometry was monitored at 280 nm using a Lambda-Max spectrophotometer (Waters). Protein concentrations for each purification step were determined using the BCA protein assay kit (Pierce) and confirmed using Dot Blot analysis. Coomassie staining of proteins in analytical SDS-polyacrylamide gel electrophoresis confirmed the high degree of purity of the GC's. Proteins migrated at approximately 29 kDa on a 12% polyacrylamide gel (Fig. 1).

2.7. Immunoblot analysis

For the Western blot, protein samples were solubilized in Laemmli sample buffer (62 mM Tris–HCl, 2% SDS, 5% β-mercaptoethanol, 10% glycerol, 0.001% bromophenol blue, pH 6.8) and heated at 100 °C for 3 min. Electrophoresis was

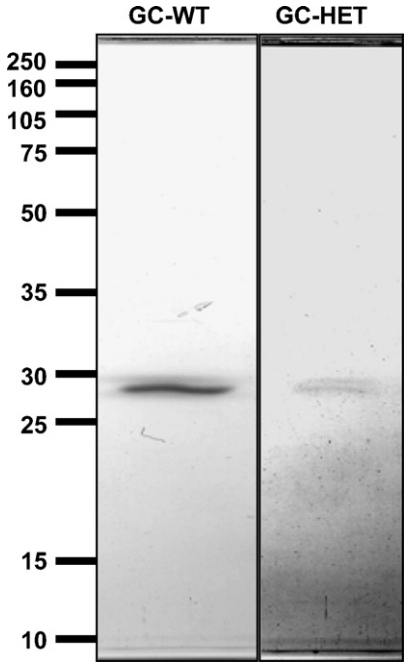

Fig. 1 – SDS-PAGE analysis of purified pGC constructs. Purified pGC enzymes (GC-WT and GC-HET) were subjected to SDS-PAGE on a 12% polyacrylamide gel and stained with Coomassie Blue, as described in Section 2.

performed in 10% polyacrylamide gel and proteins were transferred to a nitrocellulose membrane (Bio-Rad) using the liquid Mini Trans-Blot (Bio-Rad). Detection of GC's was achieved using an affinity-purified antibody from a rabbit polyclonal antiserum raised against the C-terminal sequence of the particulate guanylyl cyclase NPRA. Specific signal was probed with a horseradish peroxidase-coupled secondary antibody, according to the ECL Western blotting analysis system (Amersham Biosciences). For the Dot Blot, proteins were boiled for 3 min in 6 M urea and blotted on nitrocellulose using the Bio-Dot Apparatus (Bio-Rad). Detection of GC's was performed as described above.

2.8. Guanylyl cyclase activity

Assays were performed in a final volume of 100 μL buffer containing 25 mM HEPES, pH 7.4, 50 mM NaCl, 0.1% BSA and an excess of 4 mM $MgCl_2$ or $MnCl_2$. Purified guanylyl cyclases, GTP, nucleotides or analogs were added as indicated in the results section. No GTP regenerating system or phosphodiesterase inhibitor was added since they were not needed with pure enzyme preparation. After 10 min incubation at 37 °C, reactions were stopped by the addition of 500 μL of 110 mM zinc acetate followed by 500 μL of 110 mM sodium carbonate [17]. Tubes were then centrifuged at 12,000 × *g* for 2 min and 50 μL of supernatant was radio-immunoassayed for cyclic GMP content [18]. Concentrations of cGMP were corrected for the recovery, using an external standard of cGMP processed in the same manner throughout the steps. The recovery of cGMP varied from 60 to 70%.

2.9. Statistical analysis

Statistics were performed by ANOVA, followed by multiple comparisons using the Student–Newman–Keuls test, with $p < 0.05$ as the significance level. Values presented in figures correspond to the average and standard error of the mean from duplicates. Parameter estimates presented in tables are averages of values obtained in replicate experiments involving two separate batches of purified GC catalytic domain. Curve fitting of enzyme kinetics data for substrate and inhibitors was performed by non-linear least squares regression using the program AllFit [19]. For substrate enzyme kinetics, the curves for the time course of product formation (v) as a function of substrate concentration (S) were therefore analyzed according to Hill's equation:

$$v = \frac{V_{max} S^{n_H}}{S_{0.5}^{n_H} + S^{n_H}}$$

where $S_{0.5}$ is the equivalent of the Michaelis–Menten coefficient for cooperative kinetics, V_{max} the maximum enzyme production rate and n_H is the Hill's coefficient. For inhibition curves, data where then analyzed according to the equation:

$$v = \frac{v_0}{1 + (I/IC_{50})^n}$$

where v_0 is the initial rate of product formation in the absence of inhibitor, I the concentration of inhibitor, IC_{50} the inhibitor concentration at the midpoint of the curve and n is the slope factor for the inhibition curve. Estimation of apparent inhibition constants for inhibitors was obtained according to Segel [20]. K_i estimates were calculated using:

$$K_i = \frac{I}{((V_{max}/V^*_{max})(S^*_{0.5}/S_{0.5})) - 1}$$

where $S^*_{0.5}$ and V^*_{max} are the estimates for the $S_{0.5}$ and the V_{max} in the presence of the inhibitor at concentration I.

3. Results

3.1. Purified guanylyl cyclase domain of pGC (GC-A) is fully active

The structure of pGC or sGC catalytic domain has not yet been experimentally determined. But the crystal structure of the rat type II adenylyl cyclase C2 catalytic domain was used to obtain a molecular model. pGC was proposed to form an active dimer with two active sites by complementation of the two identical GC moieties [8]. A hinge region preceding the catalytic domain is providing a coiled-coil which favours dimerization and which was shown to be required for catalytic activity [21]. In addition, the kinase homology domain located upstream of the hinge helical region is an ATP binding site which allosterically modulates catalytic activity [5,22] and which could potentially bind other purine nucleotides. In order to specifically study the regulation of purine nucleotides on GC catalysis, we generated a truncated mutant containing only the hinge helical region and the guanylyl cyclase catalytic domain of GC-A. The mutant GC-WT was expressed in Sf9 insect cells and purified to homogeneity (Fig. 1). GC-WT was expected to be fully active because it has been shown that when the kinase-like domain of NPR-A is deleted by mutagenesis, the resulting receptor protein displays high constitutive guanylyl cyclase activity [23]. However, this activity is independent of the agonist ANP and its stimulation by ATP is abolished [23]. Thus, this truncated mutant should represent the full catalytically active form of pGC. Consistent with this model, we found that this GC-WT construct was constitutively active and stable. When cGMP production was assessed as a function of GTP concentration, we obtained a V_{max} of 28 ± 2 μmol/mg/min and a $S_{0.5}$ of 0.37 ± 0.07 mM (Table 1). GC-WT remained fully active when stored at −80 °C for 1 year. The specific activity observed was therefore favourably comparable to that reported for ANP + ATP-activated full-length GC-A expressed and purified from Sf9 insect cells (4.3 μmol cGMP formed/mg/min) [17]. Most experiments were performed using Mg^{2+} as the divalent cation as it is the natural cellular divalent cation and also because enzyme kinetics profiles of sGC or adenylyl cyclase can be very different in the presence of other divalent cations [13,24]. In fact, when we measured cGMP production using Mn^{2+}-GTP as substrate, kinetic parameters were drastically different. The $S_{0.5}$ was reduced 22-fold and the V_{max} was reduced 1.5-fold (Table 1).

3.2. Positive cooperativity in GC-WT domain

Kinetic analysis of cGMP production for the GC-WT construct also yielded a Hill slope of 1.4 ± 0.01 and an upward concave

Table 1 – Kinetic parameters of GC-WT compared to mutated proteins $D^{849}A$, $N^{968}S$ and GC-HET

	$S_{0.5}$ (mM)	n_H	V_{max} (μmol/mg/min)	$k_{cat}/S_{0.5}$ (M^{-1} s^{-1})
GC-WT	0.37 ± 0.07 (3)	1.4 ± 0.01 (3)	28 ± 2 (3)	8.5 ± 2.2 × 10^4 (3)
GC-WT (Mn^{2+}-GTP)	0.017 (0.016–0.018)	1.8 (1.7–1.9)	19 (18–20)	1.2 × 10^6 (1.1–1.3)
GC-D^{849}A	ND	ND	ND	ND
GC-N^{968}S	0.068 (0.055–0.082)	ND	0.32 (0.25–0.39)	4.8 × 10^2 (4.7–4.9)
GC-HET	0.068 ± 0.004 (5)	1.0 ± 0.06 (5)	4.1 ± 0.6 (5)	6.4 ± 0.8 × 10^4 (5)

The $S_{0.5}$ and V_{max} values were determined by kinetic analysis using Hill's equation. Production of cGMP was assessed with increasing concentration of the substrate GTP in the presence of excess Mg^{2+} unless otherwise stated, as described under Section 2. Values are mean ± S.E. of three to five separate experiments (indicated in parenthesis), with each measurement done in duplicate. When only two separate experiments are presented, both individual values are indicated in parenthesis. n_H is the cooperativity index and GC-HET is the double mutant $D^{849}A/N^{968}S$; ND, cannot be determined.

double reciprocal, which suggests positive cooperativity (Fig. 2). This is consistent with the enzyme having two active sites for GTP. We then wondered what would happen to this apparent cooperativity if pGC only had one active site.

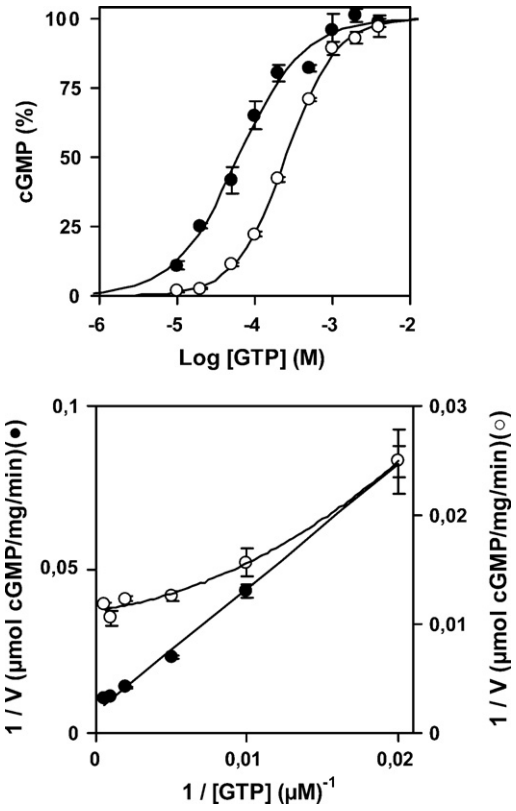

Fig. 2 – Kinetic analysis of GC-WT and GC-HET. Purified GC-WT (0.03 ng, open circle) and GC-HET (0.2 ng, closed circle) enzyme kinetics were measured as a function of GTP concentration. Mg^{2+} was present at 4 mM excess relative to GTP. Estimates of the kinetic parameters $S_{0.5}$, V_{max} and n_H were obtained by non-linear least squares using Hill's equation. The curves are portrayed as log-linear plot (upper panel) or Lineweaver–Burk double reciprocal (lower panel). cGMP production is expressed as 100% of maximum (V_{max}) for each curve. V_{max} for GC-WT and GC-HET was 28 and 4.1 μmol/mg/min, respectively. Assays were conducted as described in Section 2. The results are representative of at least three separate replicate experiments.

Two mutually complementary mutations were used to selectively inactivate one catalytic site in a heterodimeric pGC. In the model described for adenylyl cyclase, the residue Asp^{396}, present only in C1a domain, stabilizes an Mg^{2+} or Mn^{2+} ion required for binding the phosphate chain of ATP and PPi. It also stabilizes the transition state [25]. Mutation of this residue results in an approximately 1800-fold drop in enzyme catalytic efficacy. $S_{0.5}$ is 8-fold higher while V_{max} is 210-fold lower [25]. Also, the residue Asn^{1025} present only in C2 domain stabilizes the transition state [11,25,26]. Mutation of this residue results in a 40-fold reduction of V_{max}, with no change in $S_{0.5}$ [26]. Those two residues are located on separate domains C1 and C2. Once combined as a hetero-complex, they contribute to the single catalytic site of adenylyl cyclase, while the other pseudo-site is catalytically inactive, but is the site for forskolin binding. This pseudo-site could potentially be occupied by nucleotides in the absence of forskolin. A similar conformation is observed in sGC [3,15]. Indeed, it was recently documented that sGC displays both a high affinity and a low affinity binding site for nucleotides [4].

In GC-WT, the corresponding residues Asp^{849} and Asn^{968} are conserved in both GC subunits. Two active sites could then be formed when the GC subunits assemble in a head-to-tail conformation. Thus, to yield only one active site, we co-expressed the mutants GC-D^{849}A and GC-N^{968}S, including a Protein C tag or a histidine tag, respectively, to allow selective purification of the heterodimer (GC-HET) by sequential purification on Ni-NTA agarose and anti-Protein C agarose (Fig. 1). GC-D^{849}A and GC-N^{968}S homodimers were also expressed and purified to homogeneity (data not shown). The D^{849}A mutation completely abolished guanylyl cyclase activity (Table 1). The N^{968}S mutation yielded a protein almost 180-fold less catalytically active than the GC-WT, with a $S_{0.5}$ increased almost 2-fold and a V_{max} reduced 88-fold. The heterodimer (GC-D^{849}A-N^{968}S or GC-HET) showed catalytic activity similar to GC-WT, i.e. $k_{cat}/S_{0.5}$ values were not significantly different (Table 1). The $S_{0.5}$ was improved 5.5-fold but the V_{max} was reduced 7-fold. When cGMP production of GC-HET was plotted against Mg-GTP concentration, we found a Hill slope of 1.0 ± 0.06 and a linear double reciprocal plot, suggesting that the GC-HET has lost the cooperative catalytic behaviour observed for GC-WT (Fig. 2 and Table 1). These results show that two functional GTP binding sites are required for the cooperative catalytic process.

3.3. *Structure–activity profile of P-site inhibition of GC-WT by nucleosides*

Adenylyl cyclase is strongly inhibited by P-site inhibitors. Characteristic of potent P-site inhibitors is their higher potency observed in the presence of inorganic pyrophosphate [11]. It has been proposed that pyrophosphate, which is produced along with cAMP during catalysis, stabilizes a dead-end complex of adenylyl cyclase with the inhibitor [11]. It has been shown that soluble guanylyl cyclase is inhibited by 2′d3′GMP [15,27], and by physiological concentrations of ATP (1–2 mM) [28]. However, no detailed structure–activity relationships of inhibition by purine derivatives have been reported for pGC. Since pGC is homodimeric with two active sites, inhibition patterns of pGC purine derivatives might depart from those for sGC and adenylyl cyclase, which provide only a single active site. We therefore explored inhibition of GC-WT catalytic activity by commercially available adenosine and guanosine analogs. Each nucleoside was examined in experiments where guanylyl cyclase activity was measured with varying concentrations of the nucleoside, with or without adding a cellular concentration of inorganic pyrophosphate (0.3 mM) [29]. IC_{50} measured for each inhibitor is shown in Table 2. Inhibition curves in the presence of pyrophosphate are shown in Fig. 3. Pyrophosphate alone was characterized by an IC_{50} of 1.4 mM. ATP showed a weak IC_{50} of 3.3 mM, and addition of pyrophosphate did not improve its IC_{50}. Pyrophosphate did not improve inhibition by 2′d5′AMP or 2′d5′GMP (Table 2), and no inhibition was observed with 2′d3′AMP, with or without pyrophosphate. However, four guanosine containing compounds tested were potentiated when pyrophosphate was present. 2′3′-Dideoxyguanosine, guanosine, the isomer mixture guanosine-2′(3′)-monophosphate, and 2′d3′GMP were all potentiated when 0.3 mM pyrophosphate was present, improving their IC_{50} 2–8-fold (Table 2). The best inhibition for the available compounds was obtained with 2′d3′GMP in the presence of pyrophosphate (0.083 mM; Table 2). These experiments indicate that guanosine analogs of P-site agents inhibit pGC with micromolar potency. Favourable characteristics include a guanine moiety, a 2′-deoxy, the absence of 5′-phosphate and the presence of 3′-phosphate. The results are in agreement with P-site inhibition of adenylyl cyclase by adenosine analogs [10].

Further analysis reveals that 2′d3′GMP behaves as a mixed non-competitive inhibitor (Fig. 4). 2′d3′GMP dose-dependently increases the $S_{0.5}$ for GTP ($p < 0.01$). Pyrophosphate at 0.3 mM also increases the $S_{0.5}$ for GTP ($p < 0.05$). In addition, pyrophosphate potentiates the effect of 2′d3′GMP on $S_{0.5}$ from 2.3 to 8.7-fold ($p < 0.01$). On the other hand, both 2′d3′GMP and pyrophosphate decrease the V_{max} for GTP ($p < 0.01$ for both agents). However, pyrophosphate does not potentiate the inhibitory effect of 2′d3′GMP on V_{max} (26% versus 17% decrease, NS). From this data the estimated K_i for 2′d3′GMP alone is 0.49 ± 0.01 mM (Fig. 4A) and 0.068 ± 0.015 mM in the

Table 2 – Inhibition of particulate guanylyl cyclase domain by nucleosides and inorganic pyrophosphate

	IC_{50} (mM)	
	Control	+0.3 mM PPi
PPi	1.4 (1.3–1.4)	–
2′AMP	>5 (2)	ND
3′AMP	>5 (2)	ND
5′AMP	>5 (2)	ND
Adenosine	>5 (2)	ND
2′3′-Dideoxyadenosine	>5 (2)	ND
2′d3′AMP	>5 (2)	>5 (2)
ATP	3.3 (3.1–3.5)	5.3 (5.2–5.4)*
2′d5′AMP	2.3 (1.5–3.0)	1.9 (1.5–2.3)
5′GMP	>5 (2)	ND
2′d5′GMP	1.8 (1.3–2.3)	2.2 (1.5–2.8)
2′3′-Dideoxyguanosine	2.2 ± 0.53 (3)	1.0 ± 0.094 (3)*
Guanosine	2.9 (2.4–3.3)	0.38 (0.34–0.41)*
Guanosine-2′(3)′-monophosphate	1.1 (0.94–1.3)	0.30 (0.21–0.38)*
2′d3′GMP	0.43 ± 0.07 (3)	0.083 ± 0.014 (3)**

Inhibition of purified GC-WT was determined as described under Section 2 by including 1 mM GTP and varying concentrations of indicated nucleotides in the presence of excess Mg^{2+}. Activity was also determined in the presence of a physiological concentration of pyrophosphate (300 μM). Values are mean ± S.E. of three separate experiments (indicated in parenthesis), with each measurement done in duplicate. When only two separate replicate experiments are presented, both mean values are indicated in parenthesis.

* $p < 0.05$.

** $p < 0.01$.

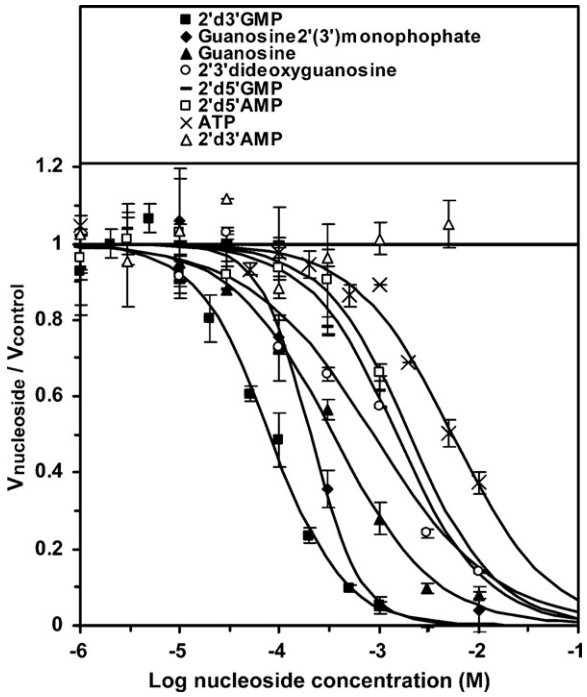

Fig. 3 – Structure–activity relationships for the inhibition of pGC. Purified GC-WT was incubated as indicated in Section 2 with 1 mM GTP, 0.3 mM inorganic pyrophosphate and increasing concentrations of indicated nucleosides. Values represent averages from at least two normalized experiments for each compound, each assayed in duplicate. IC_{50} values from these and other compounds are shown in Table 2.

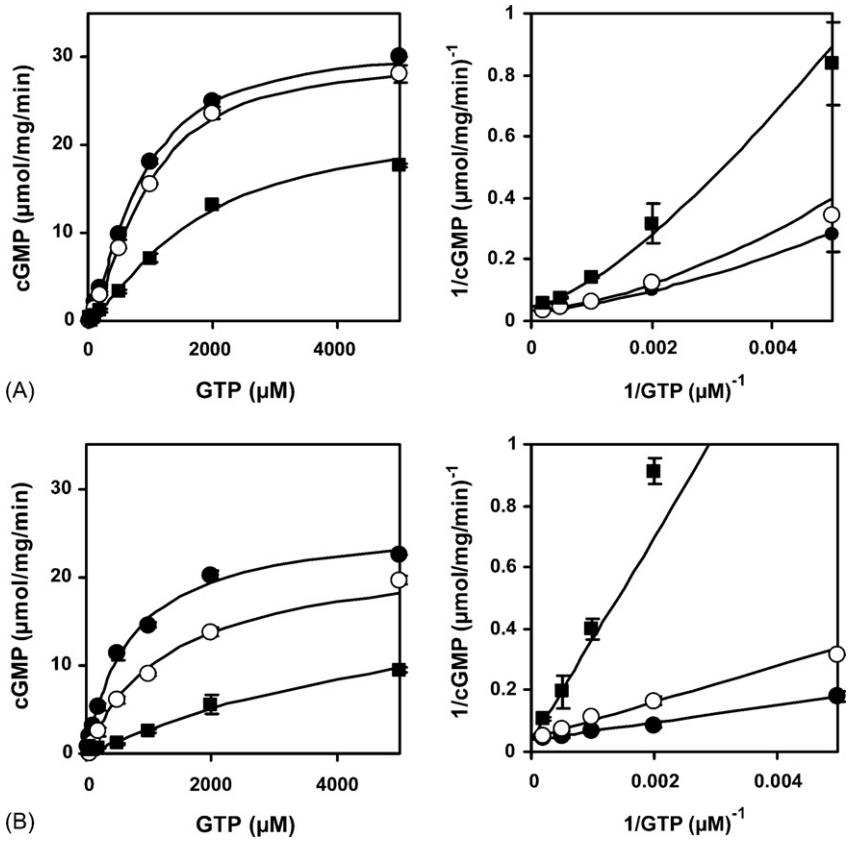

Fig. 4 – Kinetic analysis of inhibition by 2′d3′GMP. (A) GC-WT (0.03 ng) kinetic profile was measured in the absence (closed circles) or in the presence of 0.1 mM (open circle) or 1 mM (closed squares) 2′d3′GMP, using Mg-GTP as substrate. (B) GC-WT (0.03 ng) kinetic profile was measured under the same conditions as in panel (A), but with the addition of 0.3 mM pyrophosphate. The results are representative of at least three separate replicate experiments. Both experiments (A and B) are portrayed as linear (left) or double reciprocal plots (right). Enzyme kinetic analysis for each experiment was used to obtain estimated K_i values.

presence of PPi (Fig. 4B). In the presence of 2′d3′GMP alone, the kinetic curves remain positively cooperative ($n_H = 1.5 \pm 0.01$) with curvilinear double reciprocal plots (Fig. 4A). The presence of pyrophosphate attenuates or abrogates ($p < 0.05$) the positive cooperativity ($n_H = 1.1 \pm 0.06$) of the enzyme kinetics, as documented by the linear double reciprocal plots (Fig. 4B).

3.4. *2′d3′GMP P-site mixed inhibition requires only one active site*

To further investigate the mechanism of 2′d3′GMP P-site inhibition on pGC, we compared its inhibitory effect on GC-WT (two active sites) and GC-HET (one active site). Inhibition curves with and without added pyrophosphate were obtained for GC-WT and GC-HET (Fig. 5). The IC_{50} values found for GC-HET (0.38 ± 0.06 mM without added pyrophosphate and 0.072 ± 0.002 mM with pyrophosphate; Fig. 5B) were similar to the values found for GC-WT (0.43 ± 0.07 mM in the absence of pyrophosphate and 0.083 ± 0.014 mM with pyrophosphate (Table 2 and Fig. 5A). Dixon plots shown to the right in Fig. 5 indicate that in each case the slope is increased when pyrophosphate is added, documenting that pyrophosphate greatly improves the effect of 2′d3′GMP and reduces to a great extent the estimated K_i. These results indicate that 2′d3′GMP inhibition requires only one active site on pGC and that 2′d3′GMP binds directly to the active site which it inhibits. Binding of GTP or 2′d3′GMP to the inactive site is however not excluded.

4. Discussion

Positively cooperative GC enzyme kinetics in the presence of excess Mn^{2+} is a well-known property of crude or solubilized preparations of particulate guanylyl cyclase from various tissues [30–33]. A Hill slope of about 2.0 is commonly obtained [30]. Mn^{2+} was initially used in studies of sGC or pGC because guanylyl cyclase activity in enzyme preparations was often undetectable in the presence of Mg^{2+} [31]. Positively cooperative enzyme kinetics is also observed, although less pronounced, when the natural substrate Mg^{2+}-GTP is used [30,34]. Here, we demonstrate positively cooperative enzyme kinetics using Mg^{2+}-GTP with a Hill slope of 1.4, only requiring the guanylyl cyclase catalytic domain. Cooperativity was more obvious in Mn^{2+}-GTP with a Hill slope of 1.8 (Table 1). Our results also indicate that the helical hinge region and the

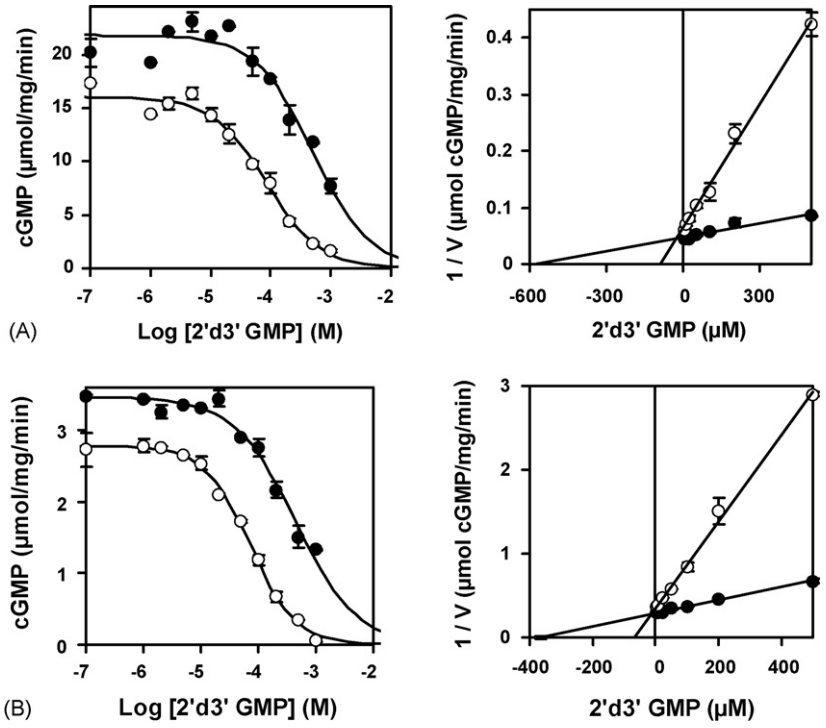

Fig. 5 – Inhibition of: (A) GC-WT and (B) GC-HET by 2′d3′GMP and pyrophosphate. GC-WT (0.03 ng) activity was measured relative to 2′d3′GMP concentration in the presence of 0.5 mM GTP and 4 mM excess of Mg^{2+}, in the absence (closed circles) or the presence (open circles) of 0.3 mM inorganic pyrophosphate. The results are representative of three separate replicate experiments. GC-HET (0.2 ng) activity was measured relative to 2′d3′GMP concentration in the presence of 0.2 mM GTP and 4 mM excess of Mg^{2+}. The results are representative of two separate replicate experiments. Results are portrayed as linear (left) and Dixon (right) plots.

catalytic guanylyl cyclase domain are sufficient to obtain a functional dimer with full cooperative properties. In the present study with pGC, Mn^{2+}-GTP behaved as a more potent substrate than Mg^{2+}-GTP. As described in the crystal structure of adenylyl cyclase, Mg^{2+} and Mn^{2+} ions generate distinct conformations of the active site. The AC-βLddATP-Mn crystal generated by Tesmer et al. shows increased electron density at the described B metal site, which contains the phosphate side chain of the nucleotide and the Mn^{2+} ion [25]. However, sGC has been shown to catalyze the formation of cAMP from ATP when Mn^{2+} is present but not with Mg^{2+} [35]. Mn^{2+} thus seems to reduce the nucleotide specificity of nucleotide cyclases by pulling the nucleotide away from the hydrophobic purine-binding pocket more towards the residues, which together with Mn^{2+}, coordinate the nucleotide phosphate chain. It is possible that reduction of both K_m and V_{max} with Mn^{2+}-GTP as substrate might be due to tighter binding of both the substrate GTP and the inhibitory by-product pyrophosphate.

Sunahara et al. previously documented that heterodimeric sGC is inhibited by 2′d3′GMP but not by 2′d3′AMP [15]. Substrate specificity between sGC and adenylyl cyclase can be exchanged by modification of two or three amino acid residues of the catalytic domain that interact with the purine moiety [27]. Interestingly, we were unsuccessful in converting the pGC (GC-A) into an adenylyl cyclase using these mutations (unpublished observations). When sGC was converted to an efficient adenylyl cyclase, specificity of P-site inhibitors was also altered, indicating that these agents target the substrate binding site of nucleotide cyclases [15]. In agreement with those reports based on heterodimeric sGC, our results indicate that P-site inhibition of homodimeric pGC is conserved in purified GC domain, and thus does not involve the nucleotide binding site of the KHD. The GC-HET construct was designed to contain mutations that inactivate one of the two potential active sites of pGC. One of these mutations ($D^{849}A$) presumably also reduced binding of inorganic pyrophosphate and of the triphosphate chain of GTP to the inactive site. This is based on the crystal structure of adenylyl cyclase in the presence of ATP analogs, which indicates that the corresponding Asp^{396} would effectively stabilize pyrophosphate binding [11,25]. The fact that P-site inhibition was equally effective on GC-HET suggests that inhibition occurs directly on the remaining active site. Although catalysis is precluded at the second active site on GC-HET, we presume that nucleotide binding might still occur with a lower affinity, because the determinants of purine binding are still present. In this respect, GC-HET closely mimics sGC conformation and could also be allosterically inhibited by nucleotide binding to the inactive pseudo-site, but with lower potency. Consistent with this idea, a recent report by Chang et al. elegantly described occupation of the non-catalytic pseudo-symmetric site of sGC by nucleotides [2]. The inhibition of sGC by ATPγS was removed by a single mutation targeting the other aspartate residue that coordinates Mg^{2+}. The mutation of two residues that are known to dictate

nucleotide selectivity also lead to a loss of allosteric inhibition [2]. Interestingly, when the enzyme kinetics parameters obtained for the GC-WT and GC-HET are compared with those for the SNAP-activated sGC [2], the V_{max} and $S_{0.5}$ values obtained for the SNAP-activated sGC more closely resemble the values obtained for GC-HET. When $S_{0.5}$ and V_{max} are compared, the GC-WT shows an 18-fold and 20-fold difference, respectively, whereas GC-HET shows only a 3-fold difference for both parameters. The reasons for these changes in K_m and V_{max} for GC-HET are not clear, although a reduction in k_{cat} would be expected to lead to a lower K_m since k_{cat} is part of the numerator of the expression for K_m. This might also suggest that pGC is a V-type cooperative dimer for which a single substrate-bound site is much less catalytic than when both sites are occupied [20]. A second binding site with lower affinity for nucleotides was recently documented for sGC [4]. This second binding is proposed to correspond to the non-catalytic pseudo-site. It is selectively competed by sGC activators like the YC-1 molecule, confirming the conclusions of Chang et al. [2].

We also document that the purified pGC catalytic domain is directly sensitive to P-site inhibition, which was initially documented for adenylyl cyclase. Since the GC domain used does not include the KHD, the potential indirect influence of nucleotides which can bind to the KHD can be excluded from these studies. Structure-function relationships for P-site inhibitors of pGC seem to be analogous to those documented for adenylyl cyclase, except for the requirement for a guanosine moiety. Inhibition of pGC by ATP is not potent in the presence of Mg^{2+}, is not increased by inorganic pyrophosphate, and is probably more typical of substrate analogs acting competitively. In contrast, 2′d3′GMP inhibition is sensitive to the addition of pyrophosphate, and behaves as an analog of the product 3′5′cGMP. P-site inhibition of adenylyl cyclase is typically considered as uncompetitive in the presence of Mg^{2+} and non-competitive when Mn^{2+} is present [11]. Thus, with the natural divalent cation Mg^{2+}, the inhibitor would presumably bind only to the enzyme–substrate or enzyme–product complex but not to the free enzyme. However, more potent P-site inhibitors with 3′-triphosphates or tetraphosphates also bind to the free enzyme and then yield a mixed non-competitive pattern [11]. Pure competitive inhibition by 2′-deoxy-3′-AMP on adenylyl cyclase has also been reported [36]. P-site inhibitors therefore seem to display variability in their apparent mechanism of inhibition [11]. For pGC, the presence of two active and cooperative sites allows for multiple interactions of 2′d3′GMP, leading to mainly a mixed non-competitive inhibition pattern. Adding inorganic pyrophosphate drastically increased inhibition by 2′d3′GMP, suggesting that 2′d3′GMP has higher affinity for the post-transition state of the enzyme bound to pyrophosphate following dissociation of cGMP. In addition, the presence of pyrophosphate reduced the cooperativity index n_H, while 2′d3′GMP only marginally altered n_H. According to the positively cooperative models B2a and B2b of Segel [20], a cooperative inhibitor is expected to reduce substrate cooperativity, while a non-cooperative inhibitor would not alter the cooperative kinetics. Thus, our results suggest that 2′d3′GMP alone does not bind cooperatively to pGC. However, inorganic pyrophosphate might contribute to retain the enzyme in a non-cooperative post-transition state, thus leading to a reduction in n_H.

P-site inhibitors of adenylyl cyclase have greatly improved over the years. Adenosine analogs with IC_{50} of about 1 μM on adenylyl cyclase were recently synthesized. The most potent compound, β-2′,5′-dideoxy-2-fluoroadenosine, showed an IC_{50} of 0.9 μM when tested on a detergent-dispersed preparation of adenylyl cyclase from rat brain [37]. Also, the pro-nucleotide inhibitor 2′,5′-dd-3′-AMP-bis(t-Bu-SATE) was engineered as a cell permeable agent and was shown to block cAMP formation in intact preadipocytes with an IC_{50} of ~30 nM [38]. Phosphorylation of the 3′-end by nucleoside phosphokinases was proposed to be an important step for potent inhibition by this molecule, although no demonstration of intracellular 3′-polyphosphate formation was documented [38]. Such membrane-permeable agents, modified to contain a guanosine moiety, could be potent guanylyl cyclase inhibitors and be useful in studies on the role of this important family of enzymes. However, P-site inhibitors so far reported appear to be either substrate or product analogs with affinity for the pre-transition or the post-transition state, respectively. Development of new analogs mimicking the transition state intermediate containing a pentacovalent phosphate [39] might also lead to a series of inhibitors with improved potency and specificity. The putative discovery of pGC-specific or sGC-specific inhibitors would be even more useful to investigate the exact role, in physiological processes, of enzymes that produce the same second messenger, cGMP. These agents could also become important in the treatment of acute pathologies where reduction of cGMP production could be beneficial, e.g. septic shock [40] or enterotoxin-induced secretory diarrhoea [41]. Moreover, these potent inhibitors could prove valuable to determine the crystal structure of guanylyl cyclases.

Acknowledgements

This work was supported by a grant from the Canadian Institutes for Health Research. S. Joubert was supported by a scholarship from Fonds de la recherche en santé du Québec.

REFERENCES

[1] Wedel BJ, Garbers DL. The guanylyl cyclase family at W2K. Annu Rev Physiol 2001;63:215–33.
[2] Chang FJ, Lemme S, Sun Q, Sunahara RK, Beuve A. Nitric oxide-dependent allosteric inhibitory role of a second nucleotide binding site in soluble guanylyl cyclase. J Biol Chem 2005;280:11513–9.
[3] Lamothe M, Chang FJ, Balashova N, Shirokov R, Beuve A. Functional characterization of nitric oxide and YC-1 activation of soluble guanylyl cyclase: structural implication for the YC-1 binding site. Biochemistry 2004;43:3039–48.
[4] Yazawa S, Tsuchiya H, Hori H, Makino R. Functional characterization of two nucleotide-binding sites in soluble guanylate cyclase. J Biol Chem 2006;281:21763–70.
[5] Padayatti PS, Pattanaik P, Ma X, Van den Akker F. Structural insights into the regulation and the activation mechanism

of mammalian guanylyl cyclases. Pharmacol Ther 2004;104:83–99.
[6] Morton DB. Invertebrates yield a plethora of atypical guanylyl cyclases. Mol Neurobiol 2004;29:97–115.
[7] Fitzpatrick DA, O'Halloran DM, Burnell AM. Multiple lineage specific expansions within the guanylyl cyclase gene family. BMC Evol Biol 2006;6–23.
[8] Liu Y, Ruoho AE, Rao VD, Hurley JH. Catalytic mechanism of the adenylyl and guanylyl cyclases: modeling and mutational analysis. Proc Natl Acad Sci USA 1997;94: 13414–9.
[9] Johnson RA, Shoshani I. Kinetics of "P"-site-mediated inhibition of adenylyl cyclase and the requirements for substrate. J Biol Chem 1990;265:11595–600.
[10] Johnson RA, Yeung SM, Stubner D, Bushfield M, Shoshani I. Cation and structural requirements for P site-mediated inhibition of adenylate cyclase. Mol Pharmacol 1989;35: 681–8.
[11] Dessauer CW, Tesmer JJG, Sprang SR, Gilman AG. The interactions of adenylate cyclases with P-site inhibitors. Trends Pharmacol Sci 1999;20:205–10.
[12] Desaubry L, Shoshani I, Johnson RA. 2′5′-Dideoxyadenosine 3′-polyphosphates are potent inhibitors of adenylyl cyclases. J Biol Chem 1996;271:2380–2.
[13] Dessauer CW, Gilman A. The catalytic mechanism of mammalian adenylyl cyclase: equilibrium binding and kinetic analysis of P-site inhibition. J Biol Chem 1997;272:27787–95.
[14] Tesmer JJG, Dessauer CW, Sunahara RK, Murray LD, Johnson RA, Gilamn AG. Molecular basis for P-site inhibition of adenylyl cyclase. Biochemistry 2000;39: 14464–71.
[15] Sunahara RK, Beuve A, Tesmer JJ, Sprang SR, Garbers DL, Gilman AG. Exchange of substrate and inhibitor specificities between adenylyl and guanylyl cyclases. J Biol Chem 1998;273:16332–8.
[16] Labrecque J, McNicoll N, Marquis M, De Léan A. A disulfide-bridged mutant of natriuretic peptide receptor-A displays constitutive activity. Role of receptor dimerization in signal transduction. J Biol Chem 1999;274:9752–9.
[17] Wong S, Ma C-P, Foster DC, Chen A-Y, Garbers DL. The guanylyl cyclase-A receptor transduces an atrial natriuretic peptide/ATP activation signal in the absence of other proteins. J Biol Chem 1995;270:30818–22.
[18] Féthière J, Meloche S, Nguyen TT, Ong H, De Léan A. Distinct properties of atrial natriuretic factor receptor subpopulations in epithelial and fibroblast cell lines. Mol Pharmacol 1989;35:584–92.
[19] De Léan A, Munson PJ, Rodbard D. Simultaneous analysis of families of sigmoidal curves: application to bioassay radioligand assay and physiological dose–response curves. Am J Physiol 1978;235:97–102.
[20] Segel IH. Enzyme kinetics: behavior and analysis of rapid equilibrium and steady-state enzyme systems. New York: John Wiley and Sons; 1993.
[21] Wilson EM, Chinkers M. Identification of sequences mediating guanylyl cyclase dimerization. Biochemistry 1995;34:4696–701.
[22] Joubert S, Jossart C, McNicoll N, De Léan A. Atrial natriuretic peptide-dependent photolabeling of a regulatory ATP binding site on the natriuretic peptide receptor-A. FEBS J 2005;272:5572–83.
[23] Chinkers M, Garbers DL. The protein kinase domain of the ANP receptor is required for signalling. Science 1989;245:1392–4.
[24] Brandwein HJ, Lewicki JA, Waldman SA, Murad F. Effect of GTP analogs on purified soluble guanylate cyclase. J Biol Chem 1982;257:1309–11.
[25] Tesmer JJ, Sunahara RK, Johnson RA, Gosselin G, Gilman AG, Sprang SR. Two-metal-ion catalysis in adenylyl cyclase. Science 1999;285:756–60.
[26] Yan S-Z, Huang Z-H, Shaw RS, Tang W-J. The conserved asparagine and arginine are essential for catalysis of mammalian adenylyl cyclase. J Biol Chem 1997;272: 12342–9.
[27] Beuve A. Conversion of a guanylyl cyclase to an adenylyl cyclase. Methods 1999;19:545–50.
[28] Ruiz-Stewart I, Tiyyagura SR, Lin JE, Kazerounian S, Pitari GM, Schulz S, et al. Guanylyl cyclase is an ATP sensor coupling nitric oxide signaling to cell metabolism. Proc Natl Acad Sci USA 2004;101:37–42.
[29] Naeger LK, Miller MD. Mechanisms of HIV-1 nucleoside reverse transcriptase inhibitor resistance: is it all figured out? Curr Opin Investig Drugs 2001;2:335–9.
[30] Ivanova K, Heim J-M, Gerzer R. Kinetic characterization of atrial natriuretic factor-sensitive particulate guanylate cyclase. Eur J Pharmacol 1990;189:317–26.
[31] Chrisman TD, Garbers DL, Parks MA, Hardman JG. Characterization of particulate and soluble guanylate cyclases from rat lung. J Biol Chem 1975;250:374–81.
[32] Radany EW, Bellet RA, Garbers DL. The incorporation of a purified membrane-bound form of guanylate cyclase into phospholipid vesicles and erythrocytes. Biochim Biophys Acta 1985;812:695–701.
[33] Ramarao CS, Garbers DL. Receptor-mediated regulation of guanylate cyclase activity in spermatozoa. J Biol Chem 1985;260:8390–6.
[34] Parkinson SJ, Carrithers SL, Waldman SA. Opposing adenine nucleotide-dependent pathways regulate guanylyl cyclase C in rat intestine. J Biol Chem 1994;269:22683–90.
[35] Gerzer R, Hofmann F, Schultz G. Purification of a soluble sodium-nitroprusside-stimulated guanylate cyclase from bovine lung. Eur J Biochem 1981;116:479–86.
[36] Johnson RA, Shoshani I. Inhibition of *Bordetella pertussis* and *Bacillus anthracis* adenylyl cyclases by polyadenylate and "P"-site agonists. J Biol Chem 1990;265:19035–9.
[37] Ye S, Rezende MM, Deng W-P, Herbert B, Daly JW, Johnson RA, et al. Synthesis of 2′5′-dideoxy-2-fluoroadenosine and 2′5′-dideoxy-25′-difluoroadenosine: potent P-site inhibitors of adenylyl cyclase. J Med Chem 2004;47:1207–13.
[38] Laux WHG, Pande P, Shoshani I, Gao J, Boudou-Vivet V, Gosselin G, et al. Pro-nucleotide inhibitors of adenylyl cyclases in intact cells. J Biol Chem 2004;279:13317–32.
[39] Tesmer JJ, Sunahara RK, Gilman AG, Sprang SR. Crystal structure of the catalytic domains of adenylyl cyclase in a complex with Gsa-GTPgS. Science 1997;278:1907–16.
[40] Hama N, Itoh H, Shirakami G, Suga S-I, Komatsu Y, Yoshimasa T, et al. Detection of C-type natriuretic peptide in human circulation and marked increase of plasma CNP level in septic shock patients. Biochem Biophys Res Commun 1994;198:1177–82.
[41] Forte Jr LR. Uroguanylin and guanylin peptides: pharmacology and experimental therapeutics. Pharmacol Ther 2004;104:137–62.